*Zootaxa* 1119: 29–58 (2006)
www.mapress.com/zootaxa/


ISSN 1175-5326 (print edition)
**ZOOTAXA**
ISSN 1175-5334 (online edition)

**1119**

# Anatomical investigation of the slender catshark *Schroederichthys tenuis* Springer, 1966, with notes on intrageneric relationships (Chondrichthyes: Carcharhiniformes: Scyliorhinidae)

ULISSES L. GOMES [1], GERHARD O. PETERS [2], MARCELO R. DE CARVALHO [3] & OTTO B. F. GADIG [4]

[1] *Universidade do Estado do Rio de Janeiro, Instituto de Biologia, Departamento de Zoologia, Rua São Francisco Xavier 524, CEP 20559-900, Rio de Janeiro, RJ, Brazil; grant from PROCIÊNCIA/UERJ/FAPERJ; e-mail: ulisses@uerj.br*

[2] *Fellowship from FAPERJ, proc. no. E-26/151.222/98*

[3] *Departamento de Biologia, Universidade de São Paulo, Av. Bandeirantes 3900, CEP 14040-901, Ribeirão Preto, SP, Brazil; e-mail: mrcarvalho@ffclrp.usp.br*

[4] *Universidade Estadual Paulista, Campus do Litoral Paulista, Unidade São Vicente – Praça Infante Dom Henrique, s/n, CEP 11330-900, São Vicente, São Paulo, Brazil; e-mail: gadig@csv.unesp.br*

## Abstract

The slender catshark *Schroedericthys tenuis* Springer, 1966, originally described from two immature males, is redescribed on the basis of 12 specimens of both sexes, juveniles and adults (as well as the holotype and paratype). The supplementary specimens were collected off the northern coast of Brazil between Amapá and Pará states. Aspects of its external morphology, color pattern, dermal denticles, dentition, vertebral counts, and the cephalic, clasper and pectoral fin skeleton are described in detail and fully illustrated. These features are compared with those of congeneric species. Our observations support preliminary results of work in progress that *S. maculatus* Springer, 1966, *S. tenuis* and *S. saurisqualus* Soto, 2003 form a monophyletic group, mostly on the basis of neurocranial morphology, and that *S. bivius* (Smith, 1838) and *S. chilensis* (Guichenot, 1848) should be removed from *Schroederichthys*.

**Key words:** *Schroedericthys tenuis*, Scyliorhinidae, anatomical description, phylogenetic relationships, western South Atlantic Ocean

## Introduction

Sharks of the genus *Schroederichthys* Springer, 1966 are small to medium-sized catsharks (Scyliorhinidae) restricted to temperate and tropical waters of South and Central America, occurring on the continental shelf and upper slope (Compagno, 1984, 1988). The genus

*Accepted by A. Gill: 2 Nov. 2005; published: 30 Jan. 2006*

was described for *Schroederichthys maculatus* (type-species) and *S. tenuis*, two small and strongly attenuated species that differed from other scyliorhinids in having a greatly elongated postpelvic trunk region and well developed upper and lower labial folds (Springer, 1966). Adults of *S. maculatus* were abundant but unknown for *S. tenuis*, for which only two specimens existed for almost 20 years since its original description and Springer's (1979) subsequent review of the Scyliorhinidae. A third specimen, an immature male 260 mm in total length, was finally collected off Suriname in waters 72 m deep (Uyeno and Sasaki, 1983). Springer's original specimens measured 230 and 180 mm total length (holotype and paratype, respectively) and were also immature males, captured off the mouth of the Amazon River in 410 m (Springer, 1966).

Springer (1979) expanded *Schroederichthys* to include the South American *Scyllium bivium* Smith, 1838 and *Scyllium chilense* Guichenot, 1848, two species that were previously assigned to either *Scyliorhinus* Blainville, 1816 (Regan, 1908; Norman, 1937) or the Indo-Pacific genus *Halaelurus* Gill, 1862 (Garman, 1913; Springer, 1966; Kato *et al*., 1967; Gosztonyi, 1973; Menni *et al*., 1979). Springer's (1979) reallocation of these species was based on the observation that newly hatched individuals of *Halaelurus bivius* were as attenuated as both species of *Schroederichthys*. In addition, Springer was informed that an unreported adult specimen of *Schroederichthys tenuis* from southeastern Brazil in the ISH collection in Hamburg differed from adult *S. maculatus* in not being attenuated (pers. comm. from the late G. Krefft; Springer, 1979), which further corroborated the assignment of *H. bivius* and *H. chilensis* to *Schroederichthys*, and led Compagno (1984) to deduce that the tapered adult body of *S. maculatus* was neotenic. The ISH/Hamburg *Schroederichthys* specimen was examined by one of us (MRC) in 1996 and identified as a new species of *Schroederichthys*, which is now referred to *S. saurisqualus* Soto, 2003[1].

New specimens of *S. tenuis* appeared only in 1991 when one male and two females were collected from off the coast of Amapá State (northern Brazil) at 450 m (Gomes and de Carvalho, 1995; Gadig *et al*., 1996; Gadig, 2001). These specimens contained in their stomachs small teleosts and benthic invertebrates, and represented the first adult specimens of *S. tenuis*. One of the females was pregnant and contained a single egg capsule in each uterus (Gomes and de Carvalho, 1995). More importantly, these adults have highly tapered bodies and are as attenuated as juveniles of *S. tenuis* and juveniles and adults of *S. maculatus*.

The present study reports nine additional specimens of *S. tenuis* from off Pará State,

1. The original description of this species was published in a private journal with limited circulation that appears, as far as we could determine, to have been predated. We decided to date this nominal species from 2003, and not 2001 as originally claimed, because 01/09/2003 is the earliest date we could find stamped on an issue of Mare Magnum 1 (1) deposited in a public library (that of the Museu de Zoologia da Universidade de São Paulo, in São Paulo). Our decision is a conservative estimate which may eventually prove to be wrong. The proper date of publication of this nominal species, and others described in the same issue, still needs to be established.

  

northern Brazil, caught during exploratory fisheries surveys of its continental slope by the Brazilian Federal REVIZEE program. Our objectives here are to describe and illustrate the skeleton and other morphological features of this rare species, based on mature and immature individuals, and compare them with congeners. Some comments on species relationships within *Schroederichthys* are also provided, anticipating results of work still in progress (de Carvalho and Gomes, in prep.).

## Materials and Methods

Measurements were taken with calipers in a straight line, point-to-point, to the nearest tenth of millimeter (mm) following Springer (1966), and are presented in Table 1 as proportions of total length (TL). Terminology for neurocranium, copulatory organs and dermal denticles were based on Leible *et al*. (1982) and Compagno (1988, 1999). Terminology for dentition followed Compagno (1988) and Herman *et al*. (1990) and is presented in Table 2. Terminology for color pattern is according to Springer (1966; see also Schott, 1964). Vertebral numbers were taken from radiographs, and were counted following the methodology of Springer and Garrick (1964) and Compagno (1988) (Table 3). Nasobasal length was used as an independent variable in cranial proportions according to Compagno (1988: fig. 6. 13) (Table 4). Description of branchial elements was based on Compagno (1973). The drawings were made using camera lucida or directly from photographs. Specimen UERJ 1106.2, a mature female, was dissected and skeletonized. Description and illustrations of claspers were based on UERJ 1106.1, a mature male. Thorough descriptions of the external morphology of *Schroederichthys* and *S. tenuis* can be found in Springer (1966, 1979) and Compagno (1984, 1988), and will not be repeated here.

Institutional abbreviations follow Leviton *et al*. (1985), with the additions of CEPNOR (Centro de Pesquisa e Gestão de Recursos Pesqueiros do Litoral Norte, Belém, Brazil). Anatomical abbreviations are listed in the Appendix.

**Material examined.** *Schroederichthys tenuis*: USNM 188052 (holotype), 230 mm TL immature male, off mouth of Amazon River, Brazil; USNM 188053 (paratype), 180 mm TL immature male, off mouth of Amazon River, Brazil; UERJ 1106.1, 407 mm TL mature male, coast of Amapá State (04º 40N, 050º 03W); UERJ 1106.2, 373 mm TL mature female, coast of Amapá State (04º 40N, 050º 03W); UFPB 1564, 372 mm TL mature female, coast of Amapá State (04º 40N, 050º 03W); CEPNOR uncatalogued (nine specimens), 455 mm TL mature male, 172 mm TL immature male, 217 mm TL immature female, 157 mm TL immature female, 442 mm TL mature male, 335 mm TL immature male, 473 mm TL mature male, 471 mm TL mature male, 440 mm TL mature female. *Schroederichthys bivius*: BMNH 1857.10.20 (holotype), 690 mm TL mature male; MNHN 1990–1020, 540 mm TL mature female, “Cape of Good Hope” (probably Cape Horn; see

  

Springer, 1979). *Schroederichthys maculatus*: USNM 185556, 320 mm TL mature female, Cape Gracias a Dios, Honduras, 16º 39N, 082º 25W. *Schroederichthys saurisqualus*: ISH 1789/68, 590 mm TL female; UERJ 1568.1, 578 mm TL mature male, coast of Paraná State; UERJ 1568.2, 588 mm TL mature male, coast of Paraná State.

**Genus *Schroederichthys* Springer, 1966**
***Schroederichthys tenuis* Springer, 1966**
(Figs. 1–38, Tables 1–5)

**Diagnosis.** A differential diagnosis of *S. tenuis* is provided by Springer (1966, 1979; see also Compagno, 1984; Compagno *et al*., 2005). The genus *Schroederichthys* is effectively diagnosed in Springer (1966, 1979) and Compagno (1984, 1988).


**FIGURES 1, 2.** Adult female of *Schroederichthys tenuis* (CEPNOR uncat., 440 mm TL) in dorsal (1) and lateral (2) views.

**Coloration.** As in most scyliorhinids, *Schroederichthys tenuis* presents both spots and saddles dorsally, and a mostly white, pale ventral surface (Figs. 1–11). The spots are smaller than eye diameter, dark, rounded, with regular diameters, and distributed both inside and around the saddles. In adults, there are numerous spots within the saddles and surrounding them from head to first dorsal fin. Juveniles have a reduced number of spots inside the saddles and fused spots around them forming continuous lines. White spots are

absent in juveniles. There are three types of saddles, primary (1), secondary (2) and subsaddles (S) (Figs. 1–4, 6–11). Primary saddles are dark, conspicuous, and without major differences between mature and immature specimens. Secondary saddles are found posterior to the first dorsal fin, and are not as dark and as well defined as primary saddles; the pre-interdorsal secondary saddle was not found in juveniles. Subsaddles are located on the paired fins below the lateral line in both adults and juveniles. The color pattern of *S. tenuis* becomes more faded with growth. The saddles have a strong and bold outline containing few rounded spots in younger specimens, but this outline seems to break with growth, becoming very weak or disappearing completely. The spots inside the saddles become more numerous and may eventually surround or outline the saddle.

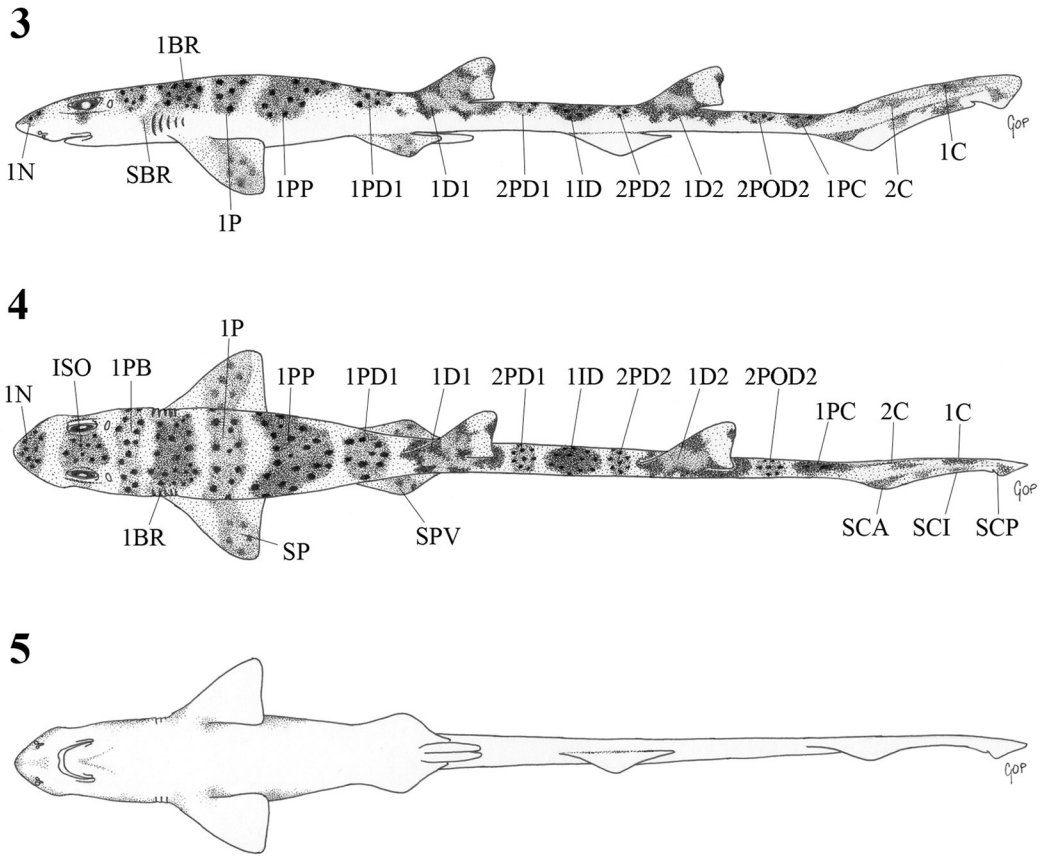


**FIGURES 3**, **4, 5.** Illustration of an adult male *Schroederichthys tenuis* (UERJ 1106.1, 407 mm TL) in lateral (3), dorsal (4), and ventral (5) views. Primary saddles are designated nasal (1N), supraorbital (1SO), prebranchial (1PB), branchial (1BR), pectoral (1P), postpectoral (1PP), pre first dorsal (1PD 1), first dorsal (1D 1), interdorsal (1ID), second dorsal (1D 2), precaudal (1PC), and caudal (1C). Secondary saddles are designated first postdorsal (2PD 1), pre-interdorsal (2PID), second dorsal (2PD 2), second postdorsal (2POD 2), and caudal (2C). Subsaddles are termed branchial (SBR), pectoral (SP), pelvic (SPV), anterior caudal (SCA), intermediate caudal (SCI), and posterior caudal (SCP).


**FIGURES 6, 7.** Holotype of *Schroederichthys tenuis* (USNM 188052, 230 mm TL, immature male) in lateral (6) and dorsal (7) views.

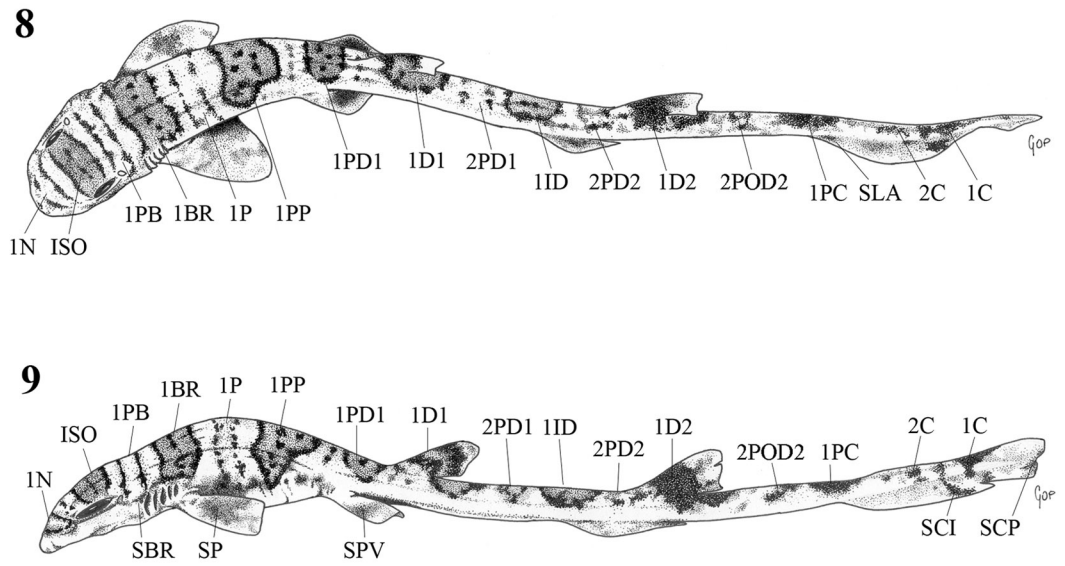


**FIGURES 8, 9.** Color pattern of *Schroederichthys tenuis* (holotype, USNM 188052, 230 mm TL, immature male) in dorsal (8) and lateral (9) views.

**Size and sexual maturity.** According to our material, male specimens of *S. tenuis* display the first signs of sexual maturity between 335–407 mm TL, as evidenced by the gradual calcification of internal clasper components, and probably reach full maturity at or before 473 mm TL. Based on material examined, the onset of sexual maturity in females seems to be between 217–373 mm TL (Gomes and de Carvalho, 1995). Sexual dimorphism is apparent in mature specimens in the shape of the mouth, which is more angular in females (Figs. 12, 13, respectively).

  

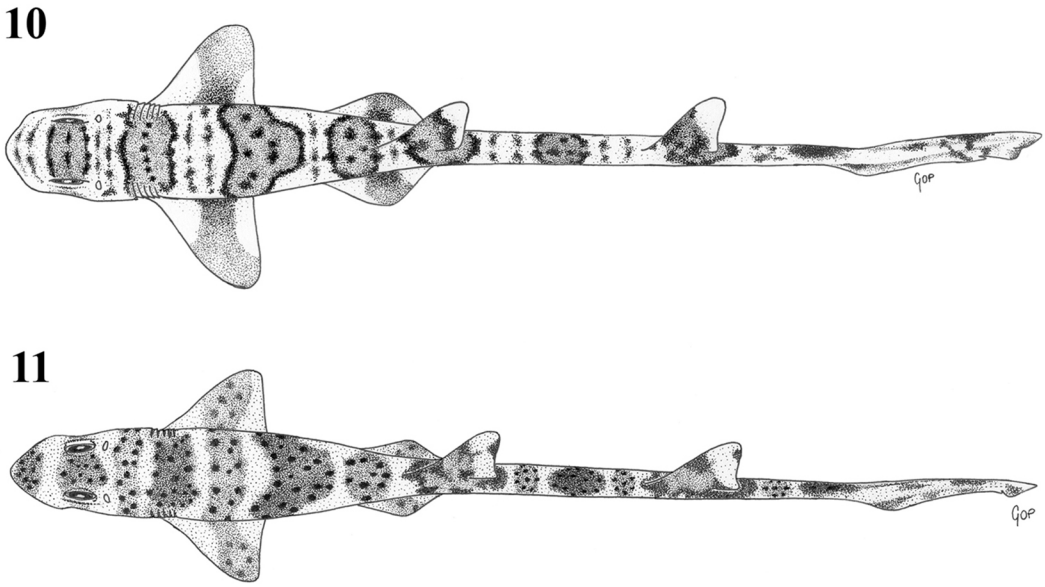


**FIGURES 10, 11.** Side-by-side comparison of immature (10) and mature (11) male specimens of *Schroederichthys tenuis* in dorsal view, showing ontogenetic changes in color pattern (based on CEPNOR specimens).

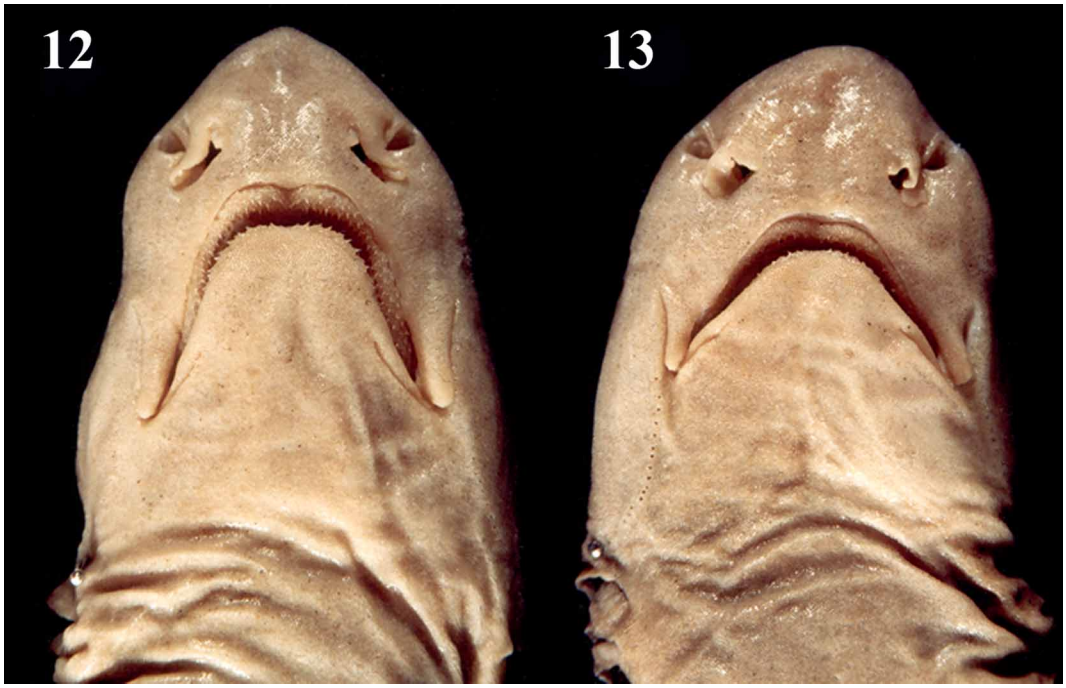


**FIGURES 12, 13.** Side-by-side comparison of ventral head region of adult male (12) (CEPNOR uncat., 473 mm TL) and adult female (13) (CEPNOR uncat., 440 mm TL) specimens of *Schroederichthys tenuis* showing sexual dimorphism; note inverted "U"-shaped mouth in 12, and "V"-shaped mouth in 13. Anterior to top.

**TABLE 1.** Measurements for specimens of *Schroederichthys tenuis* (in mm and % of TL). Mature and immature specimens refer to material from UERJ, UFPB, and CEPNOR (see material examined). Mean (*x*) and standard deviation (SD) are expressed as % of TL

| | USNM 188052 holotype | | USNM 188053 paratype | | immature specimens ( n = 12) | | mature specimens (n = 12) | | *x* | SD |
|---|---|---|---|---|---|---|---|---|---|---|
| | mm | % of TL | mm | % of TL | mm | % of TL | mm | % of TL | | |
| total length | 230.0 | | 180.0 | | 157.0–335.0 | | 372.0–473.0 | | - | - |
| orbit length | 8.0 | 3.5 | 5.0 | 2.8 | 4.0–12.0 | 2.5–3.6 | 13.0–18.0 | 3.4–4.0 | 3.4 | 0.4 |
| dist. between eye and spiracle | 3.0 | 1.3 | 2.0 | 1.1 | 2.0–3.0 | 0.9–1.3 | 3.0–4.0 | 0.7–1.0 | 0.9 | 0.2 |
| spiracle diameter | - | - | - | - | 2.0–3.0 | 0.9–1.3 | 3.0–5.0 | 0.7–1.1 | 0.9 | 0.2 |
| internasal distance | 6.0 | 2.6 | 5.0 | 2.8 | 4.0–9.0 | 2.3–3.2 | 9.0–14.0 | 2.4–3.8 | 2.8 | 0.4 |
| mouth width | 14.0 | 6.1 | 10.0 | 5.6 | 8.0–18.0 | 3.7–6.4 | 22.0–28.0 | 5.3–6.5 | 5.6 | 0.7 |
| mouth length | 6.0 | 2.6 | 4.0 | 2.2 | 3.0–13.0 | 1.9–3.9 | 12.0–23.0 | 3.2–4.9 | 3.6 | 1.0 |
| length upper labial fold | 4.0 | 1.7 | - | - | 2.0–7.0 | 1.3–2.1 | 6.0–11.0 | 1.6–2.3 | 1.9 | 0.3 |
| length lower labial fold | 5.0 | 2.2 | 3.0 | 1.7 | 2.0–5.5 | 1.2–1.8 | 5.0–9.5 | 1.3–2.0 | 1.6 | 0.3 |
| 1st gill slit width | 4.0 | 1.7 | 2.0 | 1.1 | 2.0–5.0 | 1.3–1.8 | 6.0–10.0 | 1.6–2.1 | 1.7 | 0.3 |
| 5th gill slit width | 2.0 | 0.9 | 1.0 | 0.6 | 2.0–4.0 | 1.2–1.4 | 3.0–6.0 | 0.7–1.6 | 1.1 | 0.3 |
| pelvic fin length | - | - | - | - | 11.0–28.0 | 7.0–9.7 | 40.0–43.0 | 8.7–9.5 | 8.6 | 0.9 |
| clasper inner margin length | 4.0 | 1.7 | 3.0 | 1.7 | 3.0–17.0 | 1.7–5.1 | 44.0–52.0 | 9.9–11.0 | 6.4 | 4.3 |
| dist. between dorsal fins | 44.0 | 19.1 | 33.0 | 18.3 | 31.0–68.0 | 18.9–20.3 | 73.0–96.0 | 17.5–20.7 | 19.7 | 0.9 |
| length upper lobe caudal fin | 50.0 | 21.7 | 37.0 | 20.6 | 31.0–60.0 | 17.9–19.7 | 61.0–78.0 | 15.5–18.4 | 17.9 | 1.8 |
| pelvic fin to tip of tail | 167.0 | 72.6 | 123.0 | 68.3 | 113.0–225.0 | 67.2–72.0 | 237.0–311.0 | 63.7–67.9 | 67.7 | 2.3 |
| TIP OF SNOUT TO: | | | | | | | | | | |
| anterior nasal aperture | 4.0 | 1.7 | 3.0 | 1.7 | 3.0–9.0 | 1.9–2.8 | 8.0–13.0 | 2.0–2.7 | 2.3 | 0.4 |
| posterior nasal aperture | 6.0 | 2.6 | 5.0 | 2.8 | 5.0–12.0 | 2.9–3.6 | 10.0–15.0 | 2.5–3.2 | 3.0 | 0.3 |
| mouth | 9.0 | 3.9 | 8.0 | 4.4 | 6.0–14.0 | 3.8–4.7 | 12.0–20.0 | 2.9–4.3 | 4.0 | 0.4 |
| eye | 11.0 | 4.8 | 9.0 | 5.0 | 6.0–15.0 | 3.8–5.2 | 17.0–23.0 | 4.4–5.1 | 4.8 | 0.4 |
| spiracle | 21.0 | 9.1 | 16.0 | 8.9 | 13.0–30.0 | 8.3–9.7 | 32.0–42.0 | 8.6–9.3 | 8.9 | 0.4 |
| 1st gill slit | 28.0 | 12.2 | 23.0 | 12.8 | 15.0–38.0 | 9.6–12.9 | 42.0–63.0 | 11.3–13.3 | 12.0 | 1.0 |
| 5th gill slit | 34.0 | 14.8 | 26.0 | 14.4 | 20.0–51.0 | 12.7–16.6 | 58.0–82.0 | 15.5–17.3 | 15.6 | 1.1 |
| origin pectoral | 36.0 | 15.7 | 24.0 | 13.3 | 22.0–48.0 | 14.0–15.7 | 55.0–76.0 | 14.1–16.1 | 14.8 | 0.9 |
| origin of 1st dorsal fin | 81.0 | 35.2 | 62.0 | 34.4 | 54.0–127.0 | 34.4–37.9 | 145.0–193.0 | 38.3–41.0 | 37.7 | 2.1 |
| origin of pelvic fins | 63.0 | 27.4 | 57.0 | 31.7 | 44.0–110.0 | 28.0–32.8 | 125.0–163.0 | 32.1–36.3 | 32.3 | 2.3 |
| origin of anal fin | 112.0 | 48.7 | 89.0 | 49.4 | 77.0–185.0 | 49.0–55.2 | 206.0–265.0 | 53.2–56.1 | 53.6 | 2.9 |
| anus | 68.0 | 29.6 | 53.0 | 29.4 | 48.0–114.0 | 30.6–35.5 | 127.0–171.0 | 32.3–36.3 | 33.3 | 2.3 |
| origin of 2nd dorsal fin | 133.0 | 57.8 | 100.0 | 55.6 | 91.0–210.0 | 56.7–62.7 | 197.0–299.0 | 41.8–63.2 | 59.3 | 5.7 |
| lower lobe of caudal fin | 181.0 | 78.7 | 134.0 | 74.4 | 120.0–274.0 | 76.4–81.8 | 303.0–390.0 | 79.4–83.6 | 80.4 | 2.5 |
| upper lobe of caudal fin | 186.0 | 80.9 | 146.0 | 81.1 | 125.0–276.0 | 79.6–83.7 | 303.0–403.0 | 81.2–85.6 | 82.3 | 1.6 |

*..... continued on the next page*

  

**TABLE 1** (continued)

| | USNM 188052 holotype | | USNM 188053 paratype | | immature specimens ( n = 12) | | mature specimens (n = 12) | | *x* | SD |
|---|---|---|---|---|---|---|---|---|---|---|
| | mm | % of TL | mm | % of TL | mm | % of TL | mm | % of TL | | |
| FIRST DORSAL FIN: | | | | | | | | | | |
| base | 10.0 | 4.3 | 8.0 | 4.4 | 6.0–13.0 | 3.8–5.1 | 14.0–22.0 | 3.8–5.0 | 4.4 | 0.4 |
| length free inner margin | 7.0 | 3.0 | 5.0 | 2.8 | 4.0–10.0 | 2.5–4.1 | 9.0–13.0 | 2.0–3.0 | 2.8 | 0.5 |
| height | 8.0 | 3.5 | 7.0 | 3.9 | 4.0–14.0 | 2.3–4.2 | 14.0–25.0 | 3.4–6.7 | 4.0 | 1.1 |
| length anterior margin | 9.0 | 3.9 | 14.0 | 7.8 | 13.0–28.0 | 6.9–8.4 | 31.0–36.0 | 7.4–8.8 | 7.6 | 1.2 |
| SECOND DORSAL FIN: | | | | | | | | | | |
| base | 15.0 | 6.5 | 13.0 | 7.2 | 10.0–20.0 | 6.0–7.0 | 20.0–26.0 | 4.5–6.7 | 6.0 | 0.7 |
| length free inner margin | 7.0 | 3.0 | 6.0 | 3.3 | 6.0–10.0 | 2.8–4.7 | 10.0–18.0 | 2.3–3.8 | 3.1 | 0.6 |
| height | 11.0 | 4.8 | 7.0 | 3.9 | 4.0–17.0 | 2.5–5.1 | 14.0–24.0 | 3.8–5.4 | 4.3 | 0.8 |
| length anterior margin | 21.0 | 9.1 | 16.0 | 8.9 | 15.0–29.0 | 8.7–10.1 | 21.0–44.0 | 4.8–9.4 | 8.8 | 1.3 |
| ANAL FIN: | | | | | | | | | | |
| base | 21.0 | 9.1 | 15.0 | 8.3 | 11.0–24.0 | 7.0–8.7 | 30.0–35.0 | 6.8–8.0 | 7.8 | 0.7 |
| length free inner margin | 6.0 | 2.6 | 7.0 | 3.9 | 4.0–9.0 | 2.3–3.2 | 9.0–11.0 | 2.0–2.3 | 2.6 | 0.5 |
| height | 6.0 | 2.6 | 5.0 | 2.8 | 3.0–10.0 | 1.7–3.8 | 13.0–15.0 | 2.8–3.4 | 3.0 | 0.6 |
| length anterior margin | 15.0 | 6.5 | 13.0 | 7.2 | 9.0–19.0 | 5.4–8.8 | 18.0–25.0 | 4.8–5.7 | 6.0 | 1.1 |
| PECTORAL FIN: | | | | | | | | | | |
| anterior margin | 24.0 | 10.4 | 17.0 | 9.4 | 17.0–37.0 | 10.5–12.0 | 40.0–54.0 | 10.4–11.5 | 10.9 | 0.6 |
| width at base | 19.0 | 8.3 | 6.0 | 3.3 | 5.0–13.0 | 3.2–4.1 | 12.0–17.0 | 3.2–3.7 | 3.9 | 1.3 |
| greatest width | 14.0 | 6.1 | 11.0 | 6.1 | 8.0–23.0 | 5.1–6.9 | 30.0–34.0 | 6.6–8.6 | 6.6 | 1.0 |
| DIST. BETWEEN BASES: | | | | | | | | | | |
| pectoral and pelvic fins | - | - | - | - | 24.0–50.0 | 13.8–15.3 | 58.0–75.0 | 14.1–15.9 | 14.6 | 0.6 |
| pelvic and anal fin | - | - | - | - | 27.0–62.0 | 16.6–18.5 | 74.0–90.0 | 17.0–19.5 | 18.0 | 0.9 |
| anal and lower caudal lobe | - | - | - | - | 33.0–61.0 | 18.2–22.3 | 77.0–88.0 | 17.4–19.3 | 18.9 | 1.4 |
| 2nd dorsal and upper caudal lobe | - | - | - | - | 25.0–53.0 | 15.8–16.6 | 58.0–77.0 | 13.3–16.4 | 15.4 | 1.1 |

**Dermal denticles.** Dermal denticles are divided into three regions, the denticle crown (DCR), pedicel (PED) and base (BAS) (Figs. 14, 15). In adult specimens, the crown presents an acute medial cusp (MCU). On the opposite side there are mostly four (sometimes three) medial ridges (MRI), with central ridges longer than lateral ones. On the external sides of the base of the medial ridges there are reticulated depressions (RED). The lateral expansions (LEX) are rounded (Figs. 14, 15, 18). In juveniles, the crowns present a very acute medial cusp with superficial medial ridges. Small specimens (to about 200 mm TL) present no lateral expansions, which are present in larger specimens of about 470 mm TL (Figs. 16, 17). Both adults and juveniles present short denticle pedicels and radiate

denticle bases. Dermal denticles are imbricated in adults, with the medial cusp of an anterior denticle partially covering the medial ridge of a posterior one. However, in juveniles the denticles are scattered with no superposition (Fig. 16). As shown by Springer (1966, 1979), dermal denticles change shape during ontogeny in many species of scyliorhinids, which is confirmed for *S. tenuis*.

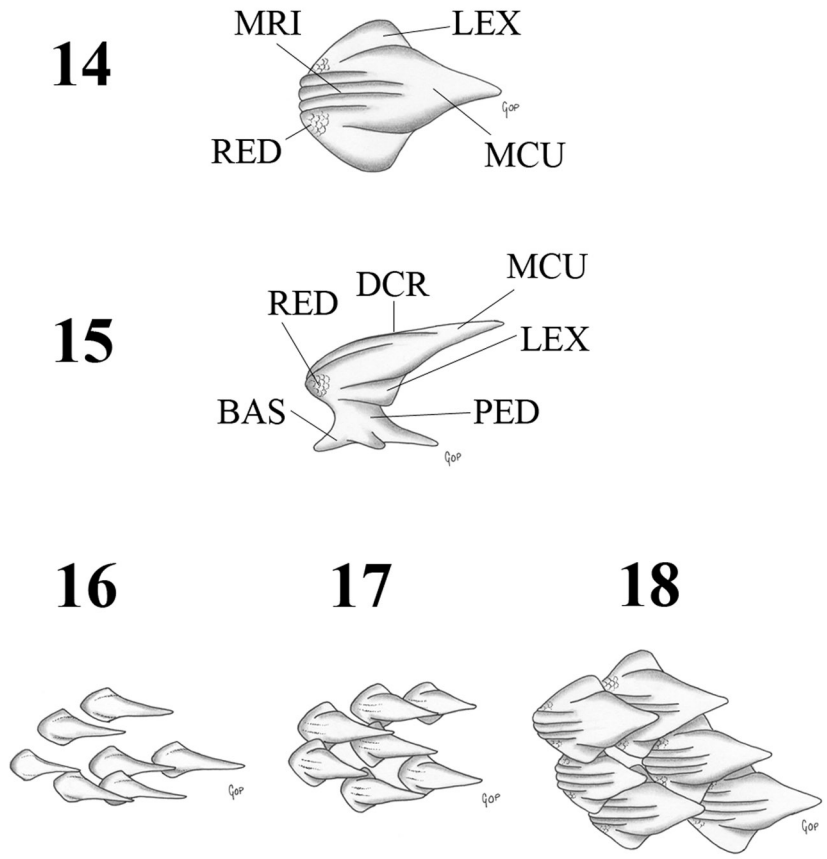


**FIGURES 14**, **15**, **16**, **17, 18.** Dermal denticles of *Schroederichthys tenuis* (denticles from region just above pectoral fin, left side). (14) mature male (CEPNOR uncat., 473 mm TL) in dorsal view. (15) same specimen in lateral view. (16) juvenile female (CEPNOR uncat., 157 mm TL) in dorsal view. (17) juvenile male (CEPNOR uncat., 217 mm TL) in dorsal view. (18) mature male (CE PNOR uncat., 473 mm TL) in dorsal view.

**Dentition.** The dentition is typically scyliorhinid, with a well-developed primary cusp (PC) flanked by two or three cusplets (PMC) on each side. There is a basal groove (BG) between the root (RT) and the crown (CR) (Figs. 19–25). The transverse ridges (TR) or striae are present on both inner and outer aspects of the cusp and cusplets. The root is secondarily anaulacorhizid, with a fully closed groove, and has two root lobes with a central foramen (CF). Monognathic heterodonty is present, as teeth near the symphisis

present well developed primary cusps (Figs. 19–21) while posterior or commissural teeth present a low primary cusp (posteriormost teeth with a very small central cusp; Fig. 25). Gynandric heterodonty was also found – the principal cusp is more slender and developed in males (Fig. 21) than in females, when corresponding teeth are compared (Fig. 22; the same condition was reported for *S. bivius* by Goztonyi, 1973). The dental formula of the three first adults captured in 1991 could not be determined due to poor preservation. The dental formula of the holotype is 44/34. Variation was detected in tooth numbers between antimeres in both upper and lower jaws; the dental formula for the nine additional specimens is 28–34 (left), 26–36 (right) / 24–28 (left), 23–28 (right) (Table 2).

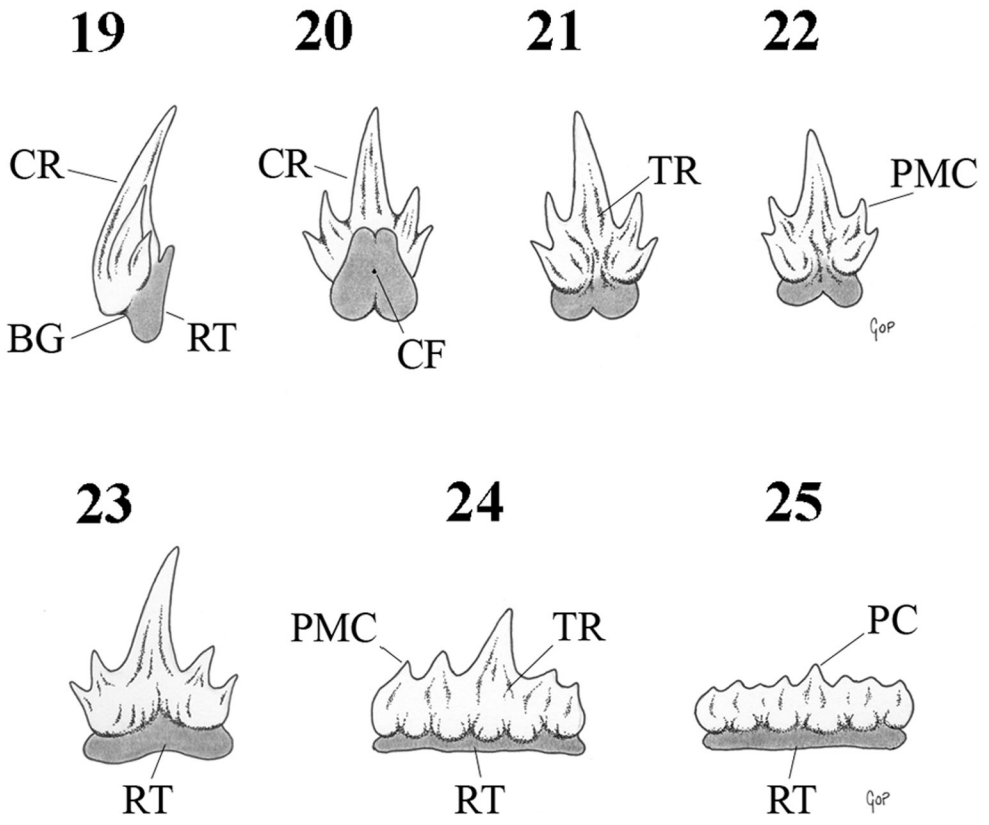


**FIGURES 19**, **20**, **21**, **22**, **23**, **24, 25.** Teeth of *Schroederichthys tenuis*. (19) inferior (3rd) tooth from right ramus in lateral view (CEPNOR uncat., 473 mm TL mature male). (20) same tooth, lingual view. (21) same tooth, labial view. (22) inferior (3rd) tooth from right ramus in labial view (CEPNOR uncat., 440 mm TL mature female). (23) inferior (8th) tooth from right ramus, labial view (CEPNOR uncat., 473 mm TL adult male). (24) inferior (21st) tooth from right ramus, labial view (same specimen). (25) inferior (31st) tooth from right ramus, labial view (same specimen).

  

**TABLE 2.** Dental formula for specimens of *Schroederichthys tenuis*. Values indicate variation in tooth number between antimeres of both jaws. All specimens from CEPNOR (uncatalogued).

| | mature male | mature female | mature female | mature male | mature female | mature male | immature female | immature female | immature female |
|---|---|---|---|---|---|---|---|---|---|
| total length (mm) | 473 | 471 | 455 | 442 | 440 | 355 | 217 | 172 | 157 |
| upper jaw | 30–31 | 32–30 | 31–30 | 28–26 | 29–28 | 30–31 | 29–30 | 34–32 | 29–26 |
| lower jaw | 24–23 | 29–28 | 28–27 | 25–26 | 25–23 | 24–26 | 24–27 | 28–28 | 25–23 |

**Vertebral counts.** Vertebral counts range from 139–150 total centra, with 32–36 monospondylous and 107–114 diplospondylous centra (Table 3). Stutter zones of alternating long and short centra were not found. No significant differences in counts were found between males and females.

**TABLE 3.** Vertebral counts of *Schroederichthys* spp.; mono = monospondylous; diplo = diplospondylous; n = number of specimens.

| Species | mono | diplo | total | source |
|---|---|---|---|---|
| *S. tenuis* (UERJ 1196.1) | 36 | 114 | 150 | present study |
| *S. tenuis* (UERJ 1196.2) | 32 | 113 | 145 | present study |
| *S. tenuis* (USNM 188052; holotype)[1] | 32 | 107 | 139 | present study |
| *S. tenuis* (USNM 188053; paratype) | 34 | 107 | 141 | present study |
| *S. bivius* (n = 1) | - | - | 153 | present study |
| *S. chilensis* (n = 2) | - | - | 135–139 | Compagno (1988) |
| *S. maculatus* (n = 32) | - | - | 132–145 | Springer (1979) |

[1] Springer (1979) reports 138 total vertebrae for the holotype.

**Head skeleton.** The head skeleton is formed by the neurocranium and visceral skeleton (jaws, labial cartilages, hyomandibulae, and branchial arches) (Figs. 26–28). The palatoquadrate (PQ) and the Meckel´s cartilage (MC) are somewhat slender. The palatine process (PP) is low and positioned behind the nasal capsule (NC). Two small and slender labial cartilages (LC) are present laterally at midjaw, and contact each other on lower jaw. The branchial arches are slightly inclined posteriorly.

*Cranial morphology.* The neurocranium is widest at nasal capsules (NC), and most narrow between orbits (OR) (Figs. 29–31; cranial measurements are presented in Table 4). Rostral cartilages are slender and not hypercalcified in adults. Lateral rostral cartilages (LR) and medial rostral cartilage (MR) are fused at their tips, forming the rostral node (RN). These three cartilages form a relatively short rostrum, with its length about one-

  

fourth of nasobasal length. Bases of lateral rostral cartilages are fused to the dorsal aspect of nasal capsules (NC) (Figs. 29–31). The nasal capsules are relatively large and somewhat oval, with broadly expanded nasal apertures (NA), and extend posteriorly from the rostral cartilages to the preorbital process (PR) dorsally and orbital notch (ON) ventrally. The anterior (precerebral) fontanelle (AF) is longer than wide, with well-defined margins, and extends anteriorly in between the nasal capsules (Fig. 29). Two small foramina are dorsolaterally situated on each nasal capsule, anterior to the preorbital process (Fig. 29). The nasal fontanelles (NF) are visible ventrally (Fig. 30).

The cranial roof extends posteriorly from the anterior fontanelle, at the level of the external foramen for the preorbital canal (FOE), to the parietal fossa (PRF) (Fig. 29). The dorsally situated external profundus nerve foramina (FPE) are smaller than the external foramen for the preorbital canal (FOE). The cranial roof is broadly arched between orbits, forming the supraorbital crests which are perfurated anteriorly by the large external foramina for the preorbital canal and the external profundus nerve foramina, and by numerous small supraorbital foramina (SOF) along the supraorbital groove (SG) (Fig. 29). The basal plate is flat, and lacks both the ectethmoid condyle and subethmoid fossa (Fig. 30), and is very narrow across the prominent orbital notches (ON). The basal plate originates behind the nasal apertures anteriorly, and extends posteriorly to the level of the stapedial foramen. The greatest width across suborbital shelves (SS), at the level of the postorbital processes (PT), is about two-thirds of nasobasal length. Two pairs of arterial foramina are present posteriorlly on the basal plate, one pair for the internal carotids (ICF) and one for the stapedial arteries (SF). The suborbital shelf is laterally straight.

The orbits are broadly oval in lateral view (Fig. 31). The orbital (or prootic) fissure (ORF) is the largest orbital foramen, located posteroventrally anterior to the otic capsule. The small orbital artery foramen (OF) is ventral to the orbital fissure, and the interorbital canal for posterior cerebral vein (IOC) is anterior to it. The foramen for the efferent spiracular artery (FES) is near the suborbital shelf, anterior to the interorbital canal. Almost directly dorsal to the efferent spiracular artery is the oculomotor nerve foramen (III). The orbitonasal foramen (ONF) is just posterior to the nasal capsule and close to the suborbital shelf. Posterior to the orbitonasal foramen is the well developed optic nerve foramen (II), and directly above it is the foramen for the anterior cerebral vein (FCV). The orbital foramen for the deep ophthalmic nerve (FPI) is located ventrally within the orbit, just dorsal to the orbitonasal foramen. The orbital foramen for the preorbital canal (FOI) is positioned more dorsally near the preorbital process. Posteriorly there are two small foramina, the trochlear nerve foramen (IV) and posterior to it the orbitocerebral foramen for the deep ophthalmic nerve (FPC). The foramen for the superficial ophthalmic nerve (FOC) is located near the postorbital process (PT).

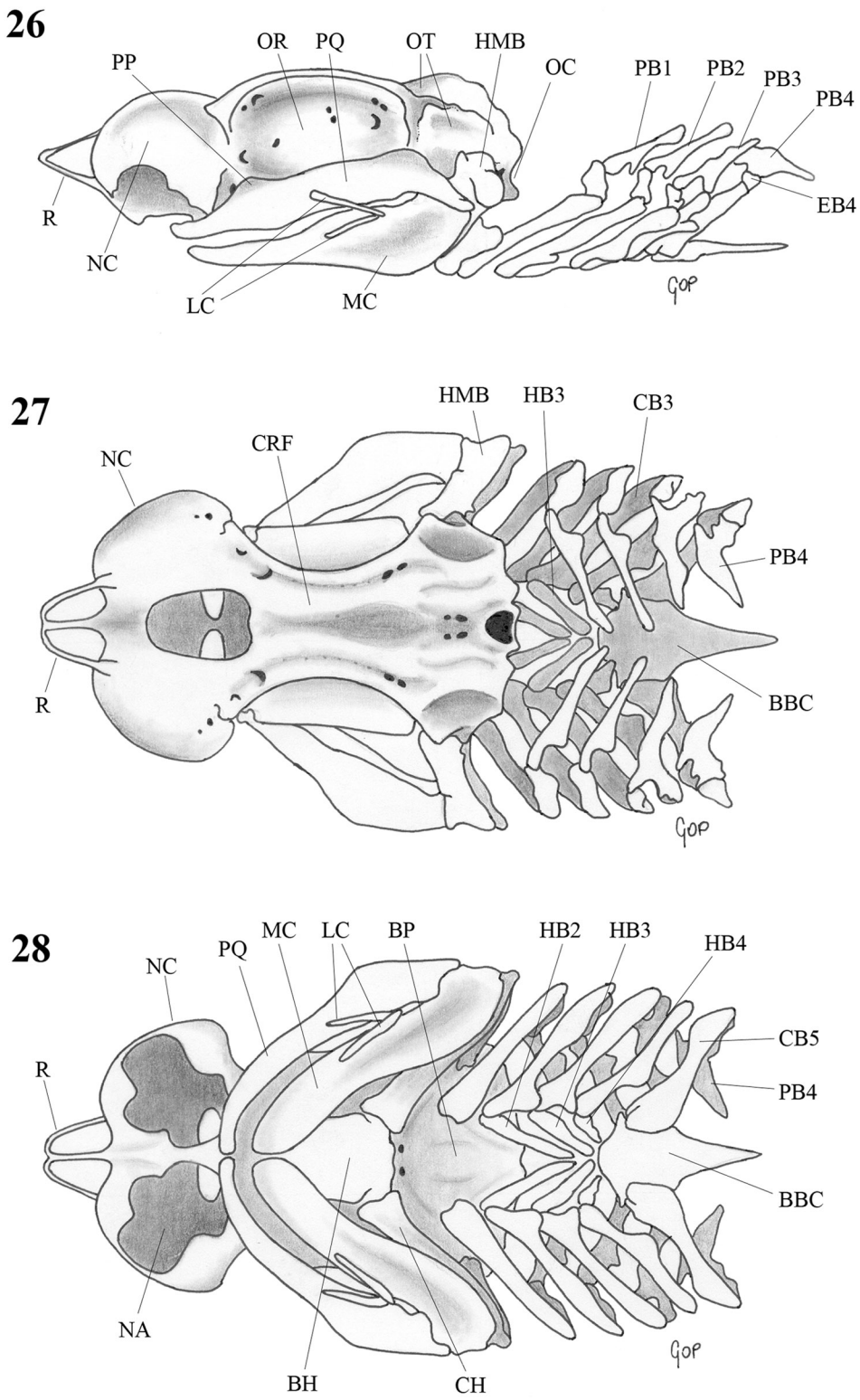


**FIGURES 26**, **27, 28.** Head skeleton of *Schroederichthys tenuis* (UERJ 1106.1, 407 mm TL, mature male) in lateral (26), dorsal (27), and ventral (28) views. Anterior to left.

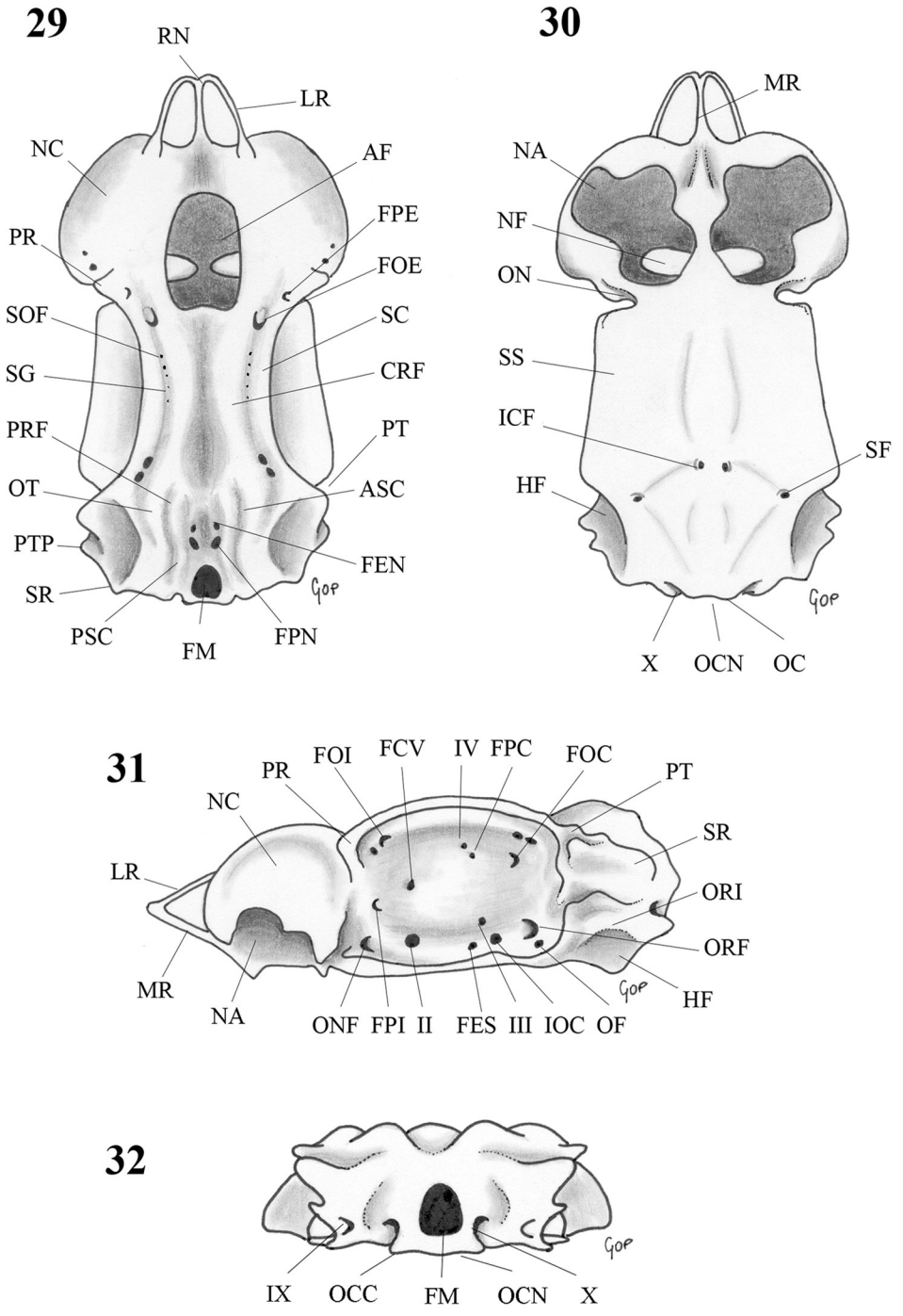


**FIGURES 29**, **30**, **31, 32.** Neurocranium of *Schroederichthys tenuis* (UERJ 1106.1, 407 mm TL, mature male) in dorsal (29), ventral (30), lateral (31), and posterior (32) views. Anterior to top in 29 and 30; anterior to left in 31.

  

**TABLE 4.** Cranial measurements of *Schroederichthys tenuis*, based on UERJ 1106.2, a 373 mm TL mature female. Measurements in mm and % of nasobasal length.

| Measurements | mm | % |
|---|---|---|
| nasobasal length | 24 | |
| rostral length | 6 | 25.0 |
| basal plate at suborbital notch level | 10 | 45.8 |
| basal plate at occipital level | 16 | 66.6 |
| least width across supraorbital crest | 8 | 33.3 |
| greatest width at nasal capsule level | 21 | 87.5 |
| width of anterior fontanelle | 5 | 20.8 |
| length of anterior fontanelle | 9 | 37.5 |
| otic capsule length | 13 | 54.1 |

The otic capsules are relatively short, located in between postorbital processes (PT) and occipital region (Figs. 29–31). The otic capsules are not greatly expanded or inflated, their greatest width just greater than one-half of nasobasal length. Dorsally on the otic capsules are the pterotic process (PTP) posterior to the postorbital process, and the sphenopterotic ridge (SR) posterior to the pterotic process. In the center of the otic capsule, the parietal fossa (PRF) bears anteriorly a pair of endolymphatic foramina (FEN) and posteriorly a pair of perilymphatic foramina (FPN). Lateral to these foramina are the anterior semicircular canals (ASC), followed by the posterior semicircular canals (PSC). Laterally, the hyomandibular facet (HF) is well defined, small and horizontally elongate. The opisthotic ridge (ORI) forms the superior margin of the hyomandibular facet. The occipital region presents low and short occiptal condyles (OCC) that do not project posteriorly, with the occipital centrum located in between (OCN). The foramen magnum (FM) is subtriangular. The vagus (X) and glossopharyngeal (IX) nerve foramina are ventrally positioned (Figs. 29, 30, 32).

*Hyomandibular and branchial skeleton*. The hyomandibular arch is formed by the hyomandibula (HMB), ceratohyal (CH), and basihyal (BH). The hyomandibula is short, about one-half as long as the ceratohyal cartilage. Its ventral extremity articulates with the ceratohyal, and its dorsal aspect articulates with the hyomandibular facet (HF) of the neurocranium (Fig. 31). The ventral portion of the ceratohyal is slightly wider than its dorsal segment, and articulates with the lateral aspect of the basyhial. The basihyal (BH) is a flat plate, widest at its posterior two-thirds, and tapers posteriorly where it contacts the ceratohyals.

The branchial arches are composed of pharyngobranchials (PB), epibranchials (EB), ceratobranchials (CB), hypobranchials (HB), and the basibranchial copula (BBC). There are four independent pharyngobranchials (PB 1-4), all directed posteriorly (Figs. 26, 27, 33). The first and second pharyngobranchials are the longest, and the fourth is the shortest.

  

The third pharyngobranchial is bifurcated at its base (probably because it incorporates the fourth epibranchial). The fourth and fifth pharyngobranchials may be fused, forming a compound posterior pharyngobranchial element. There are five epibranchials (EB 1-5); the longest are the first and second, while the shortest are the third and fifth. The fourth epibranchial is probably fused to the posterior branch of the third pharyngobranchial (Fig. 33). The five ceratobranchials (CB 1-5) are directed backwards and are about equal in length (Fig. 33). Ceratobranchials 2-3 are widest ventrally where they articulate with the hypobranchials; their ventral segments overlap the anterior portion of the subsequent ceratobranchial. Ceratobranchials 2-4 articulate with hypobranchials ventrally, but ceratobranchial 5 articulates directly with the basibranchial copula (BBC) (Fig. 33). Hypobranchials 2-4 are directed posteriorly towards the basibranchial copula. The first hypobranchial element is lacking, as is an isolated fifth hypobranchial (which is probably incorporated into the basibranchial copula). The second and third hypobranchials are longer and about equal in size, and do not touch the basibranchial copula (their posterior extremities meet each other medially); the fourth hypobranchial is the smallest and its posterior extremity articulates with the anterior portion of the basbranchial copula (Fig. 33). The basibranchial copula is flat, rounded anteriorly, and pointed posteriorly. It articulates laterally with the fourth hypobranchial and the fifth ceratobranchial (Fig. 33).

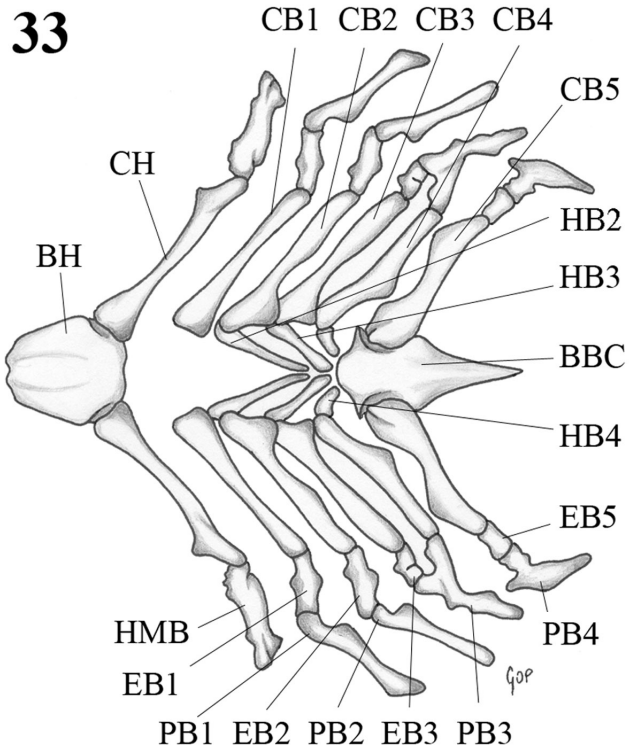


**FIGURE 33.** Branchial skeleton of *Schroederichthys tenuis* (UERJ 1106.1, 407 mm TL, mature male) in dorsal view, with dorsal elements laterally expanded. Anterior to left.

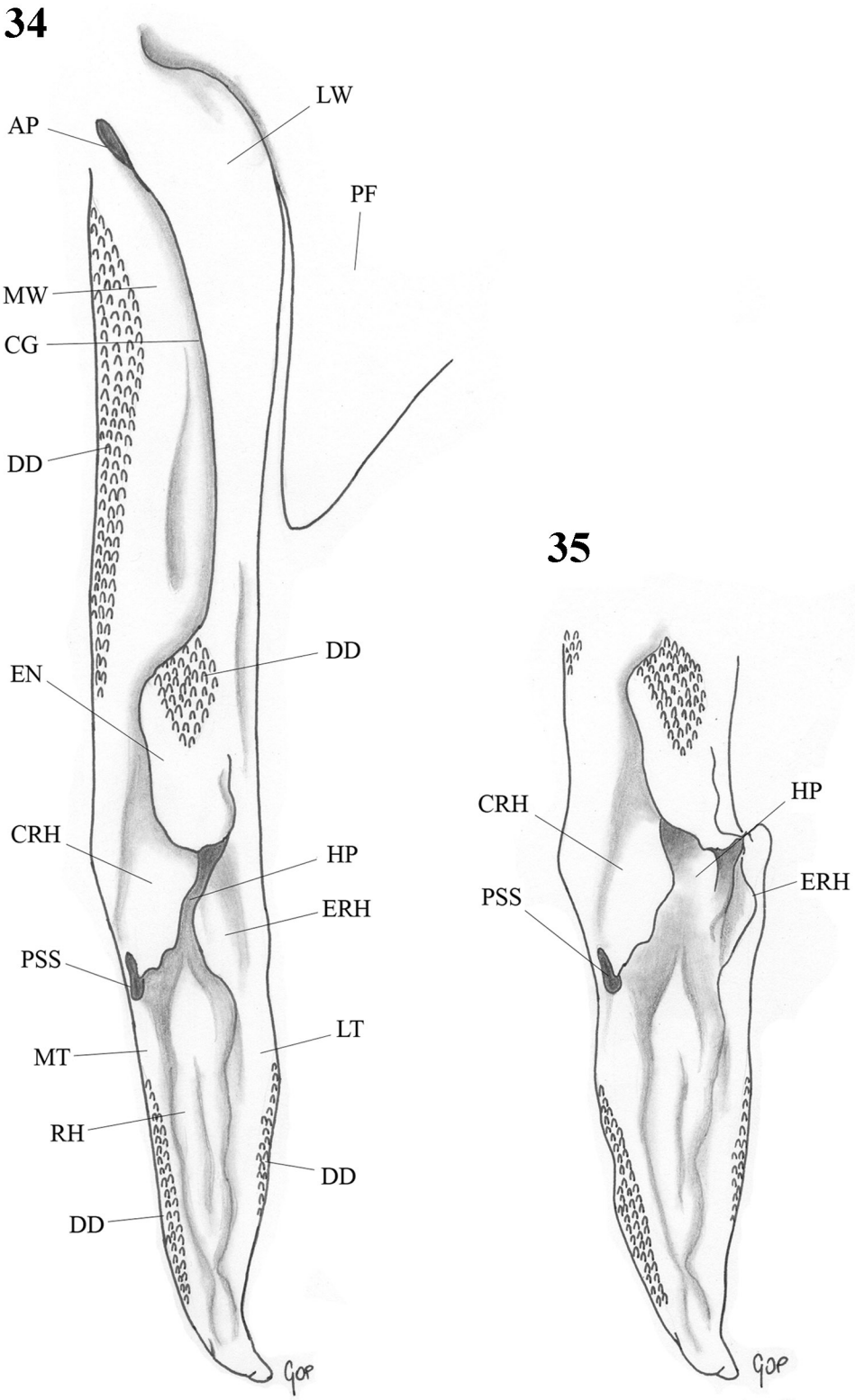


**FIGURES 34, 35.** External morphology of right clasper of *Schroederichthys tenuis* (CEPNOR uncat., 455 mm TL) in dorsal view (34), with detail of expanded glans (35). Anterior to top.

  

**Claspers.** Externally, the claspers are tubular with the glans ending in a pointed extremity. On the clasper shaft, the medial wall (MW, new term) covers the dorsal marginal cartilage (RD) while the lateral wall (LW, new term) covers the ventral marginal cartilage (RV). The clasper groove (CG) is located between the medial and lateral walls (Fig. 34). Anterodorsally, the clasper groove originates at the apopyle (AP), the receiving port of the clasper. Some structures of the external clasper glans are directly supported by skeletal components (Figs. 34, 35). The apex is formed laterally by the lateral terminal margin (LT, new term), which is supported internally by the ventral terminal cartilage, and medially by the medial terminal margin (MT, new term), which is supported by the dorsal terminal cartilage. The rhipidion (RH), situated between the lateral and ventral terminal margins, is an anteroposteriorly elongated flap on the floor of the glans, supported internally by the dorsal terminal 2 cartilage (Fig. 34). The envelope (EN), a medial extension of the lateral wall that covers part of the clasper groove, is a rounded, fleshy and soft flap with no internal support. The exorhipidion (ERH) is a longitudinally elongated and fleshy blade that covers the ventral terminal 2 cartilage and part of the ventral terminal cartilage. It is located laterally between the envelope and the lateral terminal margin (Fig. 34). The cover rhipidion (CRH) is located opposite the exorhipidion, and is an extension of the dorsomedial margin, internally supported by the accessory dorsal marginal cartilage. The pseudosiphon (PSS) is a dorsally opening, blind pocket in the posterior edge of the cover rhipidion, along the medial edge of the clasper. The hypopyle (HP) is the posterior opening of the clasper groove between the cover rhipidion and exorhipidion, anterior to the rhipidion. Dermal denticles (DD) are present on the internal side of the medial wall, envelope, and medial and lateral terminal margins, respectively (Figs. 34, 35).

A single intermediate segment (B1) and beta cartilage (β) are present dorsally in the clasper skeleton, both articulating with the basipterygium (Figs. 36, 37). In dorsal view, the preglans clasper is composed of a pair of semicylindrical marginal cartilages, the dorsal marginal (RD) and the ventral marginal (RV) (Fig. 36). The clasper groove (CG) is located in between the marginal cartilages. In ventral view, the pre-glans clasper is formed by three cartilages, with the axial cartilage (AX), an elongated and flattened rod, fused on both sides to the marginal cartilages (Fig. 37).

Five main cartilages are present in the clasper glans: ventral terminal (TV), ventral terminal 2 (TV 2), dorsal terminal (TD), dorsal terminal 2 (TD 2), and acessory dorsal marginal (RD 2) (Figs. 36, 37). The ventral terminal, the dorsal terminal and the ventral terminal 2 cartilages are lanceolate with pointed apices. The ventral terminal dorsally (Fig. 36), and the ventral terminal 2 ventrally (Fig. 37), are attached to the ventral marginal cartilage. In dorsal view, the subtriangular accessory dorsal marginal cartilage is attached to the dorsal marginal, as is the dorsal terminal cartilage ventrally. The dorsal terminal 2 cartilage lies between the accessory dorsal marginal and the ventral terminal 2, is poorly calcified, and is attached to the floor of the glans. Attached to the dorsal terminal is the small dorsal terminal acessory cartilage (TDA) (Figs. 36, 37). Four small cartilages are

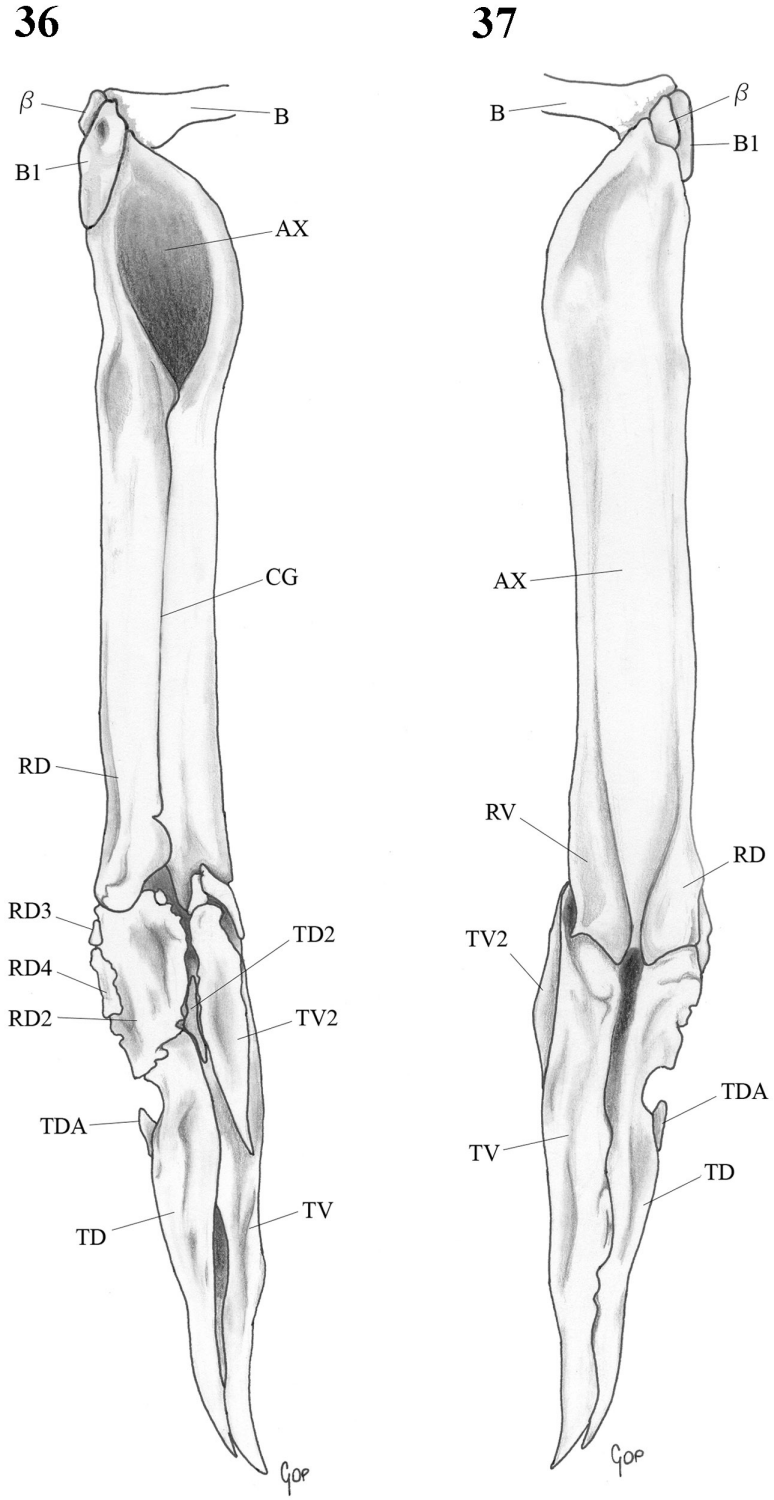


**FIGURES 36, 37.** Skeletal components of right clasper of *Schroederichthys tenuis* (UERJ 1106.1, 407 mm TL, mature male) in dorsal (36) and ventral (37) view. Anterior to top.

  

visible dorsally (Fig. 37). On the dorsal surface of the accessory dorsal cartilage there are two small elements. The anterior and smallest piece is here termed the accessory marginal cartilage 2 (RD 3). The largest element is here termed the accessory marginal cartilage 3 (RD 4), and is about three times the size of the accessory marginal cartilage 2. Both structures were found also in *S. saurisqualus*. Dorsally, between the ventral marginal and the ventral terminal 2 cartilages, are two small cartilages here designated the ventral terminal 3 (TV 3) for the internal piece, and the ventral terminal 4 (TV 4) for the external element.

**Pectoral skeleton.** The pectoral fin skeleton is aplesodic (Fig. 38) with elongated ceratotrichia, which are longer than the fin endoskeleton. The propterygium (PRO) is short with one proximal (PRA), one intermediate (IRA), and one distal (DRA) radial segment. The mesopterygium (MES) is subtriangular, and bears three proximal radial segments fused at their bases. Distally, each proximal radial articulates with one intermediate and one distal radial. The metapterygium (MET) is the largest basal cartilage, articulating with eight proximal radial segments, each with one intermediate and one distal radial segment. The metapterygial axis (MTS) is composed of shorter elements with two segments contacting the metapterygium and two distal segments. There are 12 total radial pieces (pro + meso + metapterygium) (Table 5).

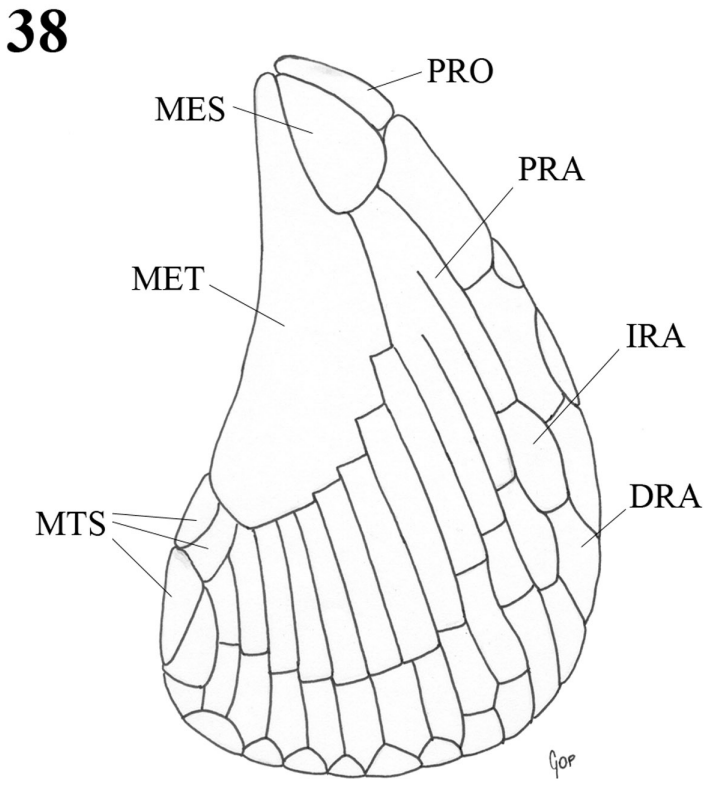


**FIGURE 38.** Right pectoral fin skeleton of *Schroederichthys tenuis* (UERJ 1106.1, 407 mm TL, mature male) in dorsal view. Anterior to top.

  

**TABLE 5.** Pectoral radial counts of *Schroederichthys* spp.; n = number of specimens.

| Species | counts | source |
|---|---|---|
| *S. bivius* (n = 1) | 15 | Nakaya (1975) |
| *S. chilensis* (n = 1) | 13 | Compagno (1988) |
| *S. maculatus* (n = 1) | 14 | Compagno (1988) |
| *S. tenuis* (n = 1) | 12 | present study |

## Results and Discussion

**Morphological comparisons.** Compagno's (1984) estimate that adults of *S. tenuis* reach 700 mm TL was based on the *Schroederichthys* specimen from southeastern Brazil deposited in Hamburg and mistakenly identified as *S. tenuis* by G. Krefft (see "Introduction" above; Springer, 1979). Specimens of this species (*S. saurisqualus*) that we examined, including the Hamburg individual, measured 578–590 mm TL, and are all sexually mature. Our observations indicate that *S. tenuis* reaches a maximum total length of probably under 500 mm, and that adults definitely have a strongly attenuated body. Species of *Schroederichthys* fall within two size classes, one for the small-sized species *S. tenuis* and *S. maculatus* (with maximum known total lengths 473 mm and 340 mm, respectively), and one including the large-sized species *S. bivius*, *S. chilensis*, and *S. saurisqualus* (reaching 700 mm TL, 620 mm TL, and 600 mm TL, respectively); we believe, however, that *S. saurisqualus* is more closely related to *S. tenuis* and *S. maculatus*, as detailed below.

According to Springer (1966, 1979) and Compagno (1988), *S. chilensis* has the highest tooth count (62/56) among congeners, with *S. maculatus* intermediate (48–53/36–42) and *S. tenuis* with the lowest number of rows (44/34 in the holotype and 26–34/23–29 in the additional specimens examined; no data were available for *S. bivius*). Gosztonyi (1973) described for *S. bivius* from Argentina the same secondary sexual dimorfism in jaw shape reported here for *S. tenuis*, which is common among scyliorhinids (Brough, 1937; Nakaya, 1975; Springer, 1979; Gomes and Tomás, 1991; Ellis and Scharley, 1995).

Vertebral counts are less reliable to separate species of *Schroederichthys*. Vertebral numbers are higher in adults of *S. tenuis* than in the type specimens (both juveniles), but this is probably artificial as counts in juveniles may be negatively affected by weaker calcification (the types of *S. tenuis* have 139–141 centra while in adults counts range from 145–150). Compared to *S. chilensis* (135–139) and *S. maculatus* (133–145), Table 3 shows no significant differences between them (data also from Springer, 1979; Compagno, 1988). A specimen of *S. bivius* (MNHN 1990-1020, a mature female) has slightly higher counts at 153 centra (33 monospondylic and 120 diplospondylic).

Neurocranial morphology is fairly distinct between *S. chilensis* and *S. maculatus*, as shown by Compagno (1988: fig. 13.6). The cranial topography of *S. tenuis* is very similar

  

to *S. maculatus* and *S. saurisqualus* in being relatively straight between the supraorbital crests, in the shape of the nasal capsules and nasal apertures, size and shape of the anterior fontanelle, width of the basal plate, and in the presence of a longitudinal groove between the anterior fontanelle and the base of the rostral cartilages between the nasal capsules (the neurocranium of *S. bivius* was not seen). Laterally, the cranial roof as well as the supraorbital crests of *S. tenuis* are both arched, but in *S. chilensis* these are straight as described by Leible *et al*. (1982).

The only description of branchial elements in other species of *Schroederichthys* is that of Leible *et al*. (1982) for *S. chilensis*, which is generally similar to *S. tenuis*. There are differences mainly in the shape and position of the basihyal (longer than wide and articulating posterolaterally with the ceratohyal in *S. tenuis*, but wider than long and overlapping the ceratohyal in *S. chilensis*). The base of the third pharyngobranchial is not bifurcated in *S. chilensis* as it is in *S. tenuis*. The basibranchial cartilage is unsegmented in *S. tenuis*, and does not articulate with the second and third hypobranchials, whereas in *S. chilensis* the basibranchial is longer, segmented, and articulates with the second to the fourth hypobranchials.

Compagno (1988) described the accessory dorsal terminal 2 cartilage in carcharhinoid sharks as being present in *Rhizoprionodon acutus*, *Halaelurus buergeri*, and *Halaelurus natalensis*. Cunha and Gomes (1994) described this structure also for *Rhizoprionodon lalandii* and *R. porosus*. In the present study the accessory dorsal terminal 2 cartilage, as well as a structure herein termed the accessory dorsal terminal 3 cartilage, were found in *Schroederichthys tenuis* and *S. saurisqualus*. Compagno (1988) affirms that the ventral terminal 2 cartilage is absent in *S. chilensis* and present in *S. maculatus*; this cartilage is present in *S. tenuis* and *S. saurisqualus* according to our observations. According to Compagno (1988), the ventral terminal 3 is present in several scyliorhinids and *Leptocharias*, and the ventral terminal 4 cartilage occurs in some *Galeus* spp. and *Halaelurus* spp. (both scyliorhinid genera). Both cartilages occur in *S. tenuis*. Compagno (1988) verified that the exorhipidion is supported internally by the ventral terminal 2 cartilage; however, both *S. tenuis* and *S. saurisqualus* have a fleshy exorhipidion without a specific endoskeletal support, and which overlies the ventral terminal and part of the ventral terminal 2 cartilages.

The arrangement of the pectoral skeleton of *S. tenuis* is similar to *S. chilensis* as described by Leible *et. al* (1982) (undescribed for *S. maculatus* and *S. bivius*). The number of radial cartilages increases from pro- to metapterygium in species of *Schroederichthys*, with *S. bivius* reaching the highest number and *S. tenuis* the lowest (Table 5). More data are required to establish if pectoral radial counts are useful to separate species of *Schroederichthys*.

**Phylogenetic relationships within *Schroederichthys*.** According to Melendez *et al*. (1993), Compagno (1999a) and Compagno *et al*. (2005), five species of *Schroederichthys* are presently recognized: *S. bivius* (Smith, 1838), *S. chilensis* (Guichenot, 1848), *S.*

*maculatus* Springer, 1966, *S. tenuis* Springer, 1966, and *S. saurisqualus* Soto, 2003. Our study supports preliminary results that *S. maculatus, S. tenuis* and *S. saurisqualus* form a monophyletic group, and that *S. bivius* (Smith, 1838) and *S. chilensis* (Guichenot, 1848) should be removed from the genus (de Carvalho and Gomes, in prep.). *S. maculatus, S. tenuis* and *S. saurisqualus*, as mentioned above, share anteroposteriorly elongated nasal apertures and nasal capsules, bulging nasal capsules that abruptly meet at their dorsal midline leaving a dorsal longitudinal groove, anteriorly oval anterior (precerebral) fontanelle with well-defined margins, presence of a small median protuberance at posterior border of anterior fontanelle, slender and laterally compressed neurocranium, slender basal plate, strongly tapered and elongated postpelvic trunk region, among other characters. These features are considered to be derived within the Scyliorhinidae, even though a posterior median protuberance is present in the anterior fontanelle of some species of *Poroderma*, *Halaelurus, Holohalaelurus,* and *Haploblepharus* (probably independently), and *Asymbolus analis* also has somewhat bulging and elongated nasal capsules, even though these are distinct from *S. maculatus, S. tenuis* and *S. saurisqualus* (Compagno, 1988). The distribution of the ventral terminal 2 cartilage, present in *S. maculatus, S. tenuis* and *S. saurisqualus*, is presently unknown within the Scyliorhinidae, as is the accessory dorsal terminal 3 cartilage, reported here in *S. tenuis* and *S. saurisqualus* (unknown for *S. maculatus*). There are also significant distinctions in the gill arch skeleton of *S. tenuis* and *S. chilensis*, but the branchial skeleton of other species of *Schroederichthys* needs to be described to reveal if it supports the monophyly of *S. maculatus, S. tenuis* and *S. saurisqualus*. The nasal flap of *S. saurisqualus* is broad and more similar to that of *S. maculatus* than to the elongated nasal flap of *S. tenuis*, but the phylogenetic significance of nasal flap morphology is questionable, as *S. bivius* has nasal flaps resembling *S. tenuis* and *S. chilensis* has nasal flaps more similar to *S. maculatus*. Gomes and de Carvalho (1995) reported that the suedelike texture, opacity and color of the egg-capsules of *S. maculatus* and *S. tenuis* was derived, a condition later found in *S. saurisqualus* but not in *S. bivius* and *S. chilensis* (Soto, 2003), further corroborating the monophyly of *S. maculatus, S. tenuis* and *S. saurisqualus*. Historically, *S. bivius* and *S. chilensis* have been placed either in *Halaelurus*, *Scyliorhinus* or *Schroederichthys* (for a review of their classification, see Springer, 1979; Compagno, 1988), but in our view their systematic fate is still undetermined within the family.

## Acknowledgments

We are grateful to the following persons for access to material under their care: R. Rosa and P. Charvet-Almeida (Universidade Federal da Paraíba), H. Wilkens, G. Schultze, and M. Stehmann (ISH), P. Pruvost (MNHN), S. L. Jewett (USNM), and P. Campbell (BMNH). J. C. Tyler (USNM) generously sent the photographs of the holotype of *S. tenuis*, and H. M. F. de Alvarenga (Museu de História Natural de Taubaté, Taubaté, Barzil)

  

took the radiographs. C. Magenta and M. Mateus (Núcleo de Pesquisa em Chondrichthyes, Santos) are thanked for providing comparative material of *Schroederichthys* spp. Diogo Pagnoncelli is acknowledged for sending photos of *S. saurisqualus*, and Murilo de Carvalho for assistance with Table 1. MRC is supported by the Fundação de Amparo à Pesquisa do Estado de São Paulo (Fapesp proc. no 02/06459-0).

## Literature Cited

Brough, J. (1937) On certain secondary sexual characters in the common dogfish (*Scyliorhinus canicula*). *Proceedings of the Zoological Society of London*, 107, 217–223.

Compagno, L.J.V. (1973) *Gogolia filewoodi*, a new genus and species of shark from New Guinea (Carcharhiniformes, Triakidae), with a redefinition of the family Triakidae and a key to triakid genera. *Proceedings of the California Academy of Sciences*, 34 (19), 383–410.

Compagno, L.J.V. (1984) FAO species catalogue. Vol.4. Sharks of the world. An annotated and illustrated catalogue of shark species known to date. Part 2. Carcharhiniformes. *FAO Fisheries Synopsis*, 125, Vol. 4 (Pt. 2), 251–655.

Compagno, L.J.V. (1988) *Sharks of the Order Carcharhiniformes*. Princeton University Press, Princeton, 486pp.

Compagno, L.J.V. (1999) Checklist of living elasmobranchs. *In*: Hamlett, W.C. (Ed.), *Sharks, Skates, and Rays*. *The Biology of Elasmobranch Fishes*. The Johns Hopkins University Press, Baltimore, pp. 471–498.

Compagno. L.J.V., Dando, M. & Fowler, S. (2005) *Sharks of the World*. Princeton University Press, Princeton, 368pp.

Cunha, M.R. & Gomes, U.L. (1994) Estudo comparativo da morfologia dos órgãos copuladores de *Rhizoprionodon lalandii* (Valenciennes, 1839) e *Rhizoprionodon porosus* (Poey, 1861) (Elasmobranchii, Carcharhinidae). *Revista Brasileira de Biologia*, 54 (4), 575–586.

Ellis, J.R. & Shackley, S.E. (1995) Ontogenetic changes and sexual dimorphism in the head, mouth and teeth of the lesser spotted dogfish. *Journal of Fisheries Biology*, 47, 155–164.

Gadig, O.B.F. (2001) *Tubarões da Costa Brasileira*. Unpubl. PhD diss. Instituto de Biociências, Universidade Estadual Paulista Júlio de Mesquita Filho, Rio Claro, 343pp.

Gadig, O.B.F., Bezerra, M.A. & Furtado-Neto, M.A.A. (1996) Novos registros e dados biológicos de tubarão-gato, *Schroederichthys tenuis* Springer, 1966 (Chondrichthyes, Scyliorhinidae) para a costa norte do Brasil. *Revista Nordestina Biologia*, 11 (1), 51–55.

Gomes, U.L. & Tomás, A.R.G. (1991) Dimorfismo sexual secundário no cação *Scyliorhinus haeckelii* Ribeiro, 1907 (Elasmobranchii, Scyliorhinidae). *Anais da Academia brasileira de Ciências*, 63 (2), 193–200.

Gomes, U.L. & de Carvalho, M.R. (1995) Egg capsules of *Schroederichthys tenuis* and *Scyliorhinus haeckelii* (Chondrichthyes, Scyliorhinidae). *Copeia*, 1995 (1), 232–236.

Gosztonyi, A.E. (1973) Sobre el dimorfismo sexual secundario en *Halaelurus bivius* (Müller & Henle, 1841) Garman, 1913 (Elasmobranchii, Scyliorhinidae) en aguas Patagonico-Fueguinas. *Physis*, Seccion A, 32 (85), 317–323.

Herman, J., Hovestadt-Euler, M. & Hovestadt, D.C. (1990) Contributions to the study of the comparative morphology of teeth and other relevant ichthyodorulites in living supraspecific taxa of Chondrichthyes fishes. Part. A.: Selachii. No 2b: Order: Carcharhiniformes - Family Scyliorhinidae. *Bulletin de l'Institute Royal de Sciences Naturalle de Belgique, Biologie*, 60, 181–230.

Last, P.R. & Stevens, J.D. (1994) *Sharks and Rays of Australia*. CSIRO, Canberra, 513pp.

Leible, M., Dittus, D.M. & Belmar, C.G.G. (1982) *Atlas Anatomico de Pintarroja Schroederichthys chilensis (Guichenot, 1848) (Chondrichthyes: Scyliorhinidae). Vol. II. Sistemas*: *Muscular, E squeletico, Respiratorio y Digestivo*. Pontificia Universidad Catolica de Chile, Talcahuano, 79 pp.

Leviton, A.E., Gibbs Jr., R.H., Heal, E. & Dawson, C.E. (1985) Standards in herpetology and ichthyology: Part I. Standard symbolic codes for institutional resource collections in herpetology and ichthyology. *Copeia*, 1985 (3), 803–832.

Melendez, R.C., Galvez, O.H. & Cornejo, A.C. (1993) *Catalogo de Coleccion de Peces Depositada en el Museo Nacional de Historia Natural de Chile*. Ministerio de Educación Publica, Direccion de Bibliotecas, Archivos y Museos. Museo Nacional de Historia Natural, Santiago, 224pp.

Nakaya, K. (1975) Taxonomy, comparative anatomy and phylogeny of Japanese catsharks, Scyliorhinidae. *Memoirs of the Faculty of Fisheries, Hokkaido Uniersity*, 23 (1), 1–94.

Schott, J.W. (1964) Chromatic patterns of the leopard shark, *Triakis semifasciata* Girard. *California Fish and Game*, 50 (2), 207–214.

Soto, J. (2003) (2001?). *Schroederichthys saurisqualus* sp. nov. (Carcharhiniformes, Scyliorhinidae), a new species of catshark from southern Brazil, with further data on *Schroederichthys* species. *Mare Magnum*, 1 (1), 37–50.

Springer, S. (1966) A review of Western Atlantic cat sharks, Scyliorhinidae, with descriptions of a new genus and five new species. *Fishery Bulletin United States Fish and Wildlife Service*, 65, 581–624.

Springer, S. (1979) A revision of the catsharks, family Scyliorhinidae. *National Oceanic and Atmospheric Administration Technical Report, NMFS Circular*, 422, 1–152.

Springer, V.G. & Garrick, J.A.F. (1964) A survey of vertebral numbers in sharks. *Proceedings of the United States Natural Museum*, 115, 559–632.

Uyeno, T. & Sasaki, K. (1983) Scyliorhinidae. *In*: Uyeno, T., Matsuura, K. & Fujii, E. (Eds.), *Fishes Trawled off Suriname and French Guiana*. Japan Marine Fishery Resource Research Center, Tokyo, pp. 52.

  

## Appendix

Anatomical abbreviations

β, beta cartilage
1, primary saddle
2, secondary saddle
II, optic nerve foramen
III, oculomotor nerve foramen
IV, trochlear nerve foramen
IX, glossopharyngeal nerve foramen
X, vagus nerve foramen
1BR, primary branchial saddle
1C, primary caudal saddle
1D1, primary first dorsal saddle
1D2, primary second dorsal saddle
1ID, primary interdorsal saddle
1N, primary nasal saddle
1P, primary pectoral saddle
1PB, primary prebranchial saddle
1PC, primary precaudal saddle
1PP, primary postpectoral saddle
1PD1, primary pre first postdorsal saddle
1SO, primary supraorbital saddle
2C, secondary caudal saddle
2PD1, secondary first postdorsal saddle
2PD2, secondary second dorsal saddle
2PID, secondary pre-interdorsal saddle
2POD2, secondary second postdorsal saddle
AF, anterior fontanelle
AP, apopyle
ASC, anterior semicircular canal
AX, axial cartilage
B, basipterygium
B1, intermediate segments
BAS, denticle base
BBC, basibranchial copula
BG, basal groove
BH, basihyal cartilage
BP, basal plate
CB, ceratobranchial cartilage
CF, central foramen
CG, clasper groove
CH, ceratohyal cartilage
CR, crown
CRF, cranial roof

  

CRH, cover rhipidion
DCR, denticle crown
DD, dermal denticles
DRA, distal radial segments
EB, epibranchial cartilage
EN, envelope
ERH, exorhipidion
FCV, anterior cerebral vein
FEN, endolymphatic foramen
FES, foramen for efferent spiracular artery
FM, foramen magnum
FOC, foramen for the superficial ophthalmic nerve
FOE, external foramen of preorbital canal
FOI, preorbital canal
FPC, foramen for the deep ophthalmic nerve
FPE, external profundus foramen
FPI, orbital foramen for the deep ophthalmic nerve
FPN, perilymphatic foramen
HB, hypobranchial cartilage
HF, hyomandibular facet
HMB, hyomandibula (epihyal)
HP, hypopyle
ICF, internal carotid foramen
IOC, interorbital canal for posterior cerebral vein
IRA, intermediate radial segments
LC, labial cartilage
LEX, lateral expansion
LR, lateral rostral cartilage
LT, lateral terminal margin
LW, lateral wall
MC, Meckel's cartilage
MCU, medial cusp
MES, mesopterygium
MET, metapterygium
MR, medial rostral cartilage
MRI, medial ridge
MT, medial terminal margin
MTS, distal segment of metapterygium (metapterygial axis)
MW, medial wall
NA, nasal aperture
NC, nasal capsule
NF, nasal fontanelle
OC, occiput
OCC, occipital condyle
OCN, occipital centrum
OF, orbital artery foramen
ON, orbital notch

  

ONF, orbitonasal foramen
OR, orbit
ORI, opisthotic ridge
ORF, orbital fissure (prootic)
OT, otic capsule
PAF, parietal fossa
PB, pharyngobranchial cartilage
PC, primary cusp
PED, denticle pedicel
PMC, mesial cusplets
PP, palatine process
PQ, palatoquadrate
PR, preorbital process
PRA, proximal radial segments
PRF, parietal fossa
PRO, propterygium
PSC, posterior semicircular canal
PSS, pseudosiphon
PT, postorbital process
PTP, pterotic process
R, rostrum
RD, dorsal marginal cartilage
RD2, accessory dorsal marginal cartilage
RD3, accessory marginal cartilage 2
RD4, accessory marginal cartilage 3
RED, reticulated depression
RN, rostral node
RT, root
RV, ventral marginal cartilage
S, subsaddle
SBR, branchial subsaddle
SC, supraorbital crest
SCA, anterior caudal subsaddle
SCI, intermediate caudal subsaddle
SCP, posterior caudal subsaddle
SF, stapedial foramen
SG, supraorbital groove
SOF, supraorbital foramen
SP, pectoral subsaddle
SPV, pelvic subsaddle
SR, sphenopterotic ridge
SS, suborbital shelf
TD, dorsal terminal cartilage
TDA, dorsal terminal acessory cartilage
TD2, dorsal terminal 2 cartilage
TR, transverse ridge
TV, ventral terminal cartilage

  

TV2, ventral terminal 2 cartilage
TV3, ventral terminal 3 cartilage
TV4, ventral terminal 4 cartilage

  